

THE PROBLEM OF DETERMINING
DEPTH OF FOCUS
WITH APPLICATIONS
TO NEVADA EARTHQUAKES

By

Roger W. Greensfelder

111

Submitted in partial
fulfillment of requirements
for the Master of Science Degree

Mackay School of Mines

University of Nevada

October, 1964

Approved by Alan S. Ryal
Director of Thesis

Approved by E. J. Ryan
Department Head

Approved by J. D. Brien
Graduate Dean

TABLE OF CONTENTS

ACKNOWLEDGEMENTS

The writer wishes to express thanks to Dr. Alan Ryall for his encouragement in the writing of this thesis, and especially for his help with the section on station delays. Dr. Ryall's computer epicenter-locating program was a great help in making depth of focus calculations, and his crustal model (with eastward-dipping Moho) was necessary to the success of this thesis. D. B. Slemmons criticized the final draft, and some of his suggestions were used. Austin Jones provided useful data on regional S-wave traveltime curves and helpful criticism of the early drafts. This work was supported by the Air Force Office of Scientific Research, under grant AF-AFOSR-646-64.

III. APPLICATIONS OF THE METHOD TO SOME REGIONAL INVESTIGATIONS

 Trough Earthquake Sequence 11

 Walker Lake Earthquake 13

 The Walker Lake Crustal Structure 15

 Western Seismicity of the Sierra and Sierra Nevada 20

TABLE OF CONTENTS

| | Page |
|--|------|
| Introduction | 1 |
| I. REVIEW OF PRINCIPLES AND METHOD OF HYPOCENTER DETERMINATION | |
| The Traveltime Curves. | 2 |
| Location of Epicenters by Means of S-P Time. | 5 |
| Hypocenter Location by S-P | 6 |
| The Method of Least Squares. | 7 |
| The Thirlaway Method | 11 |
| II. THE P_g - P_n METHOD | |
| Theoretical Considerations | 14 |
| The Necessity of an Accurate Crustal Model | 17 |
| Effect of the Surface Sedimentary Layer. | 18 |
| III. APPLICATION OF THE METHOD TO SOME NEVADA EARTHQUAKES | |
| Tonopah Earthquake Series. | 22 |
| Walker Lake Series | 23 |
| The Walker Lake Crustal Anomaly. | 23 |
| Western Boundary of the Basin and Range Province | 25 |

INTRODUCTION

A subject of fundamental importance in applied seismology is the location of an earthquake focus or hypocenter, the source of natural seismic disturbances. Precise location of foci is especially useful in understanding the tectonic process of seismic belts, and is of current interest in the underground nuclear shot detection program of the Department of Defense. While the theory of hypocenter location is straightforward, precise hypocenter solutions are very difficult to obtain in practice, due to the inhomogeneity and complexity of the earth's crust and upper mantle. In the case of shallow earthquakes, with which this thesis is concerned, depth of focus is the most difficult hypocentral parameter to determine. The reasons for this will be explained below.

The purpose of the research presented here is first to delineate the problem of depth of focus determination. This will be done through the discussion of several well-known methods and their relative merit. Secondly, one of these methods, that of the P_g minus P_n time difference, will be refined and applied to some Nevada earthquakes. The particular method chosen was dictated by the fact that seismograph stations in Nevada are few and widely spaced, ruling out the use of other procedures which require four or more stations very close to the epicenter. Furthermore, the U. S. Geological Survey has completed many refraction profiles in Nevada, so that crustal structure is well-enough known here to make the P_g - P_n method feasible.

I. REVIEW OF PRINCIPLES AND METHODS OF HYPOCENTER DETERMINATION.

The Traveltime Curve. The basis of most practical work in seismology is the traveltime curve, which gives the traveltime of a seismic wave phase as a function of distance along the earth's surface. Generally time is plotted on the ordinate and distance on the abscissa. Figure 1 shows a typical set of traveltime curves for near earthquakes (epicentral distance less than 100 km) which occur at the earth's surface. There are four curves on this graph, representing the four major wave phases generated by a near earthquake: P_n , P_g , S_n , S_g . The fact that the slopes are different is due to the different velocities of these phases. P-waves are compressional (longitudinal) waves, and S-waves are shear (transverse) waves, and the velocity of each wave type is a function of the elastic parameters of the media through which it travels.

The phases P_n and P_g were first discovered in 1909 by A. Mohorovicic, although he designated P_g by \bar{P} . (Richter, 1958, p. 282). Mohorovicic found that up to a critical distance of from 100 to 150 km from the epicenter, the first P arrival is a strong, sharp impulse followed by smaller motion; past the critical distance the first arrival, designated P_n , is relatively small and contains low frequency vibrations, and is followed by larger and higher frequency wave motion. This later sharp phase Mohorovicic called \bar{P} and he identified it with the sharp first arrival seen at distances less than the critical distance. These relationships may be seen on the traveltime curves of figure 1.

The surface that separates the regions of low and high velocity is called the Mohorovicic discontinuity, or simply "Moho". It is now generally believed that the Moho separates the earth's crust and mantle, and the phases P_n and S_n travel at the base of the Moho while P_g and S_g travel within the crystalline crust (see fig. 1). Evidence for this correlation between wave

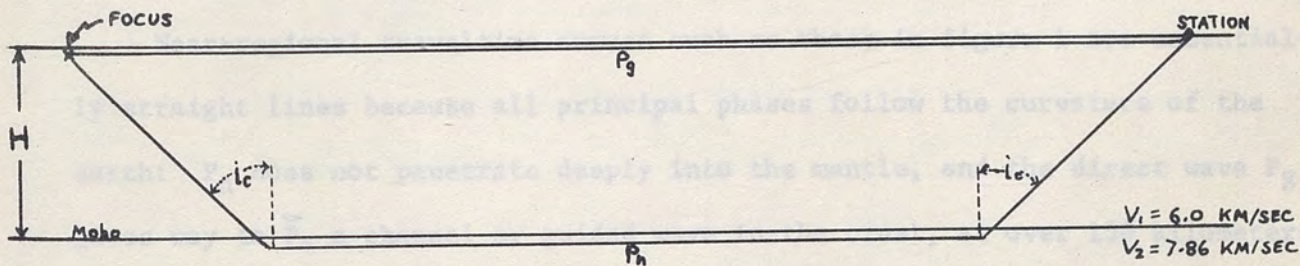
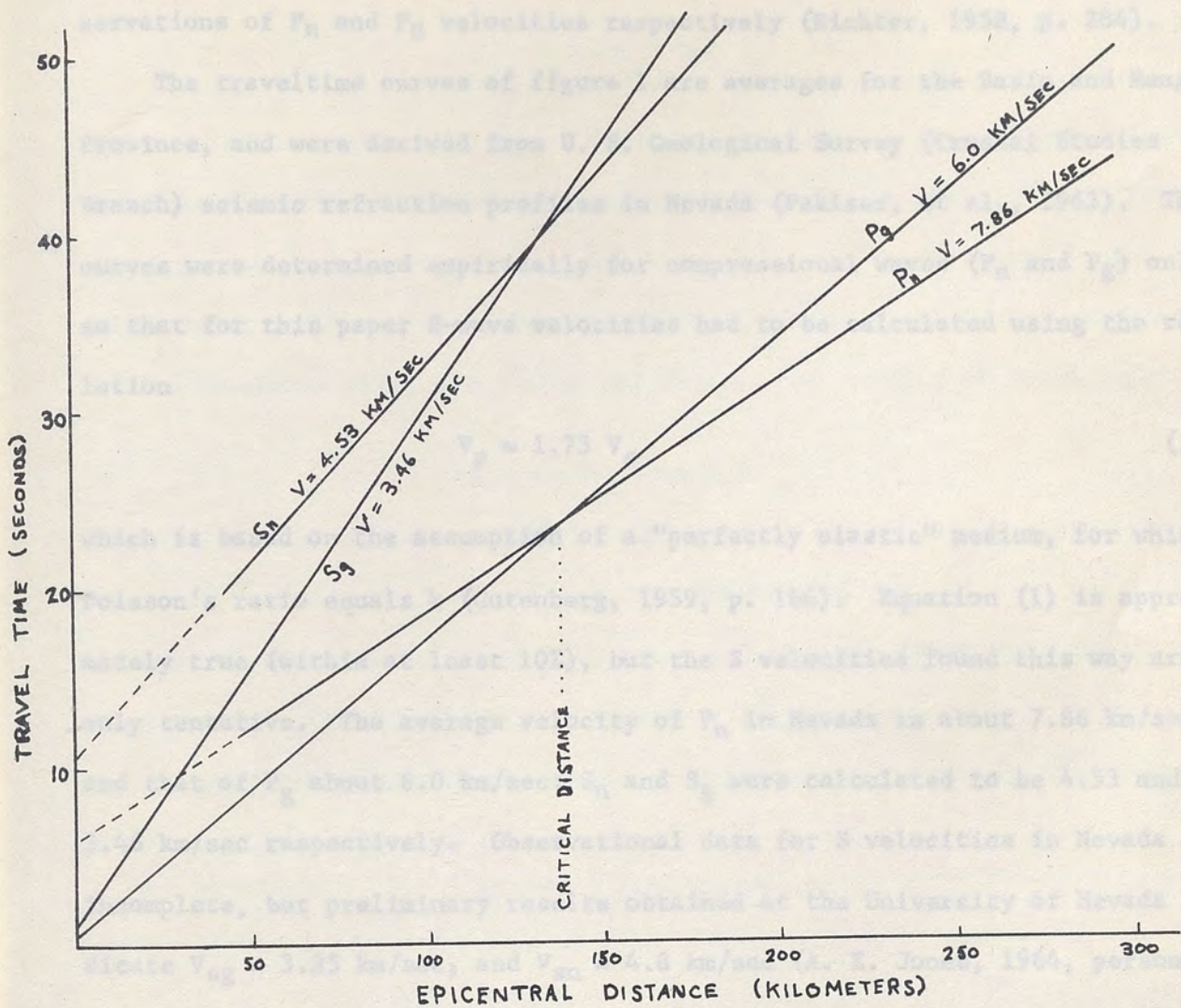


Fig. 1 Travel time curves for a surface focus and ray-path diagram.

velocities and path is drawn from laboratory experiments on the velocity of sound in granite and dunite under high pressures; dunite shows a velocity of 8 km/sec, and granite about 6 km/sec, corresponding with seismological observations of P_n and P_g velocities respectively (Richter, 1958, p. 284).

The travelttime curves of figure 1 are averages for the Basin and Range Province, and were derived from U. S. Geological Survey (Crustal Studies Branch) seismic refraction profiles in Nevada (Pakiser, et al., 1963). The curves were determined empirically for compressional waves (P_n and P_g) only, so that for this paper S-wave velocities had to be calculated using the relation

$$V_p = 1.73 V_s \quad (1)$$

which is based on the assumption of a "perfectly elastic" medium, for which Poisson's ratio equals $\frac{1}{4}$ (Gutenberg, 1959, p. 166). Equation (1) is approximately true (within at least 10%), but the S velocities found this way are only tentative. The average velocity of P_n in Nevada is about 7.86 km/sec, and that of P_g about 6.0 km/sec; S_n and S_g were calculated to be 4.53 and 3.46 km/sec respectively. Observational data for S velocities in Nevada are incomplete, but preliminary results obtained at the University of Nevada indicate $V_{sg} = 3.35$ km/sec, and $V_{sn} = 4.8$ km/sec (A. E. Jones, 1964, personal communication).

Near-regional travelttime curves such as those in figure 1 are essentially straight lines because all principal phases follow the curvature of the earth: P_n does not penetrate deeply into the mantle, and the direct wave P_g gives way to \bar{P} , a channel or guided wave in the crust, at over 150 kilometers epicentral distance (Richter, 1958, p. 286). \bar{P} is a wave which is thought to be due to multiple reflection within the crust, and which is continuous with P_g on the travelttime graph. P_g amplitude decays much more rapidly with distance than does P_n amplitude, so that at distances over 150 kilometers,

\bar{P} is the direct wave for all practical purposes, and will hereafter be referred to as P_g . All of these near-regional traveltimes may be expressed by an equation of the form

$$t = t_0 + \Delta/V \quad (2)$$

where t is the traveltimes, t_0 is the intercept time, Δ is epicentral distance, and V is the velocity of the wave in question. In the case of P_g there is a small intercept time (traveltimes for Δ equal 0) due to the delay in the low velocity or weathered layer at the surface. If the velocity and thickness of the weathered layer are V_0 and h_0 , then it may readily be shown that

$$t_0 = h_0/V_0 (\cos i_c), \quad (3)$$

where i_c is the critical angle of refraction at the bottom of that layer. The time t_0 for P_g is generally about $\frac{1}{2}$ second (Pakiser, et al., 1963). For a crust of constant thickness, the intercept time for P_n is just the extra time required for travel in the crust over the time necessary were the entire horizontal path length in the mantle. The equation for the P_n traveltimes curve is given by

$$t = \frac{\Delta}{V_2} + 2H \left(\frac{\sec i_c}{V_1} - \frac{\tan i_c}{V_2} \right) \quad (4)$$

or

$$t = \frac{\Delta}{V_2} + 2H \frac{\cos i_c}{V_1} \quad (5)$$

where Δ = horizontal distance from epicenter to receiver

H = crustal thickness

$i_c = \sin^{-1} (V_1/V_2)$, the critical angle of refraction

V_1 = velocity of P_g

V_2 = velocity of P_n

The same relations hold for S-waves, excepting that the velocities are dif-

ferent. It is apparent from equation (5) that intercept time is proportional to crustal thickness.

The above equations apply to a surface focus event, whose traveltime curves are as shown on figure 1. For an event with depth of focus h , the P_g traveltime curve becomes

$$t = \frac{1}{V_1} \sqrt{\Delta^2 + h^2} \quad (6)$$

which describes a hyperbola; figure 2 shows this traveltime curve for $h = 15$ km. The P_n traveltime curve becomes

$$t = \frac{\Delta}{V_2} + (2H-h) \frac{\cos i_c}{V_1} \quad (7)$$

from which it is seen that increasing the depth of focus reduces the intercept time. These facts will be used later on in the development of methods for determining depth of focus.

It should be stressed here that any traveltime curve is an average of time-distance relations over one or many paths. The U. S. Geological Survey refraction profiles (Pakiser et al., 1963) show considerable scatter of points about the best-fitting curves, in spite of the fact that both shot-point and recording control on these profiles were ideal. Hence it appears that there are inherent and unavoidable uncertainties in seismic traveltimes; this fact will be seen to be important later. On the basis of the simple, constant-thickness, one-layer crustal model, the P_n traveltime curve is a function of 5 independent variables: upper mantle velocity, crustal velocity, crustal thickness, and velocity and thickness of the weathered layer. But in spite of all these variables, one hypothesis of crustal structure may agree well with observations in a particular region (Ryall and Jones, 1964). Location of Epicenters by Means of S-P Time Differences. The simplest and oldest method of finding epicenters is to determine epicentral distances

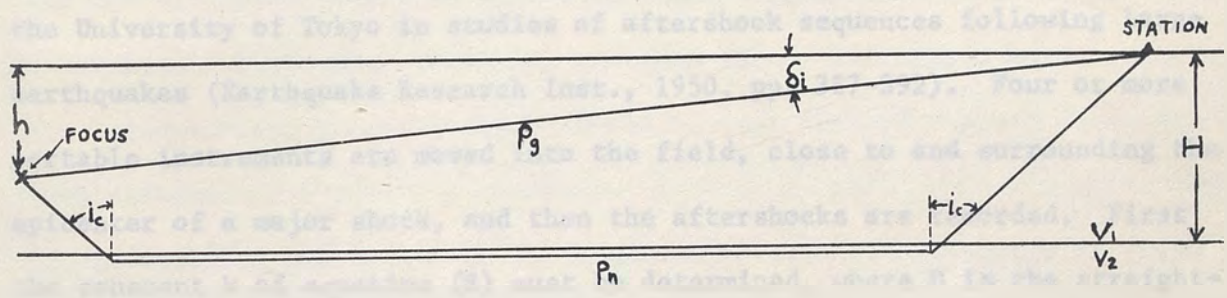
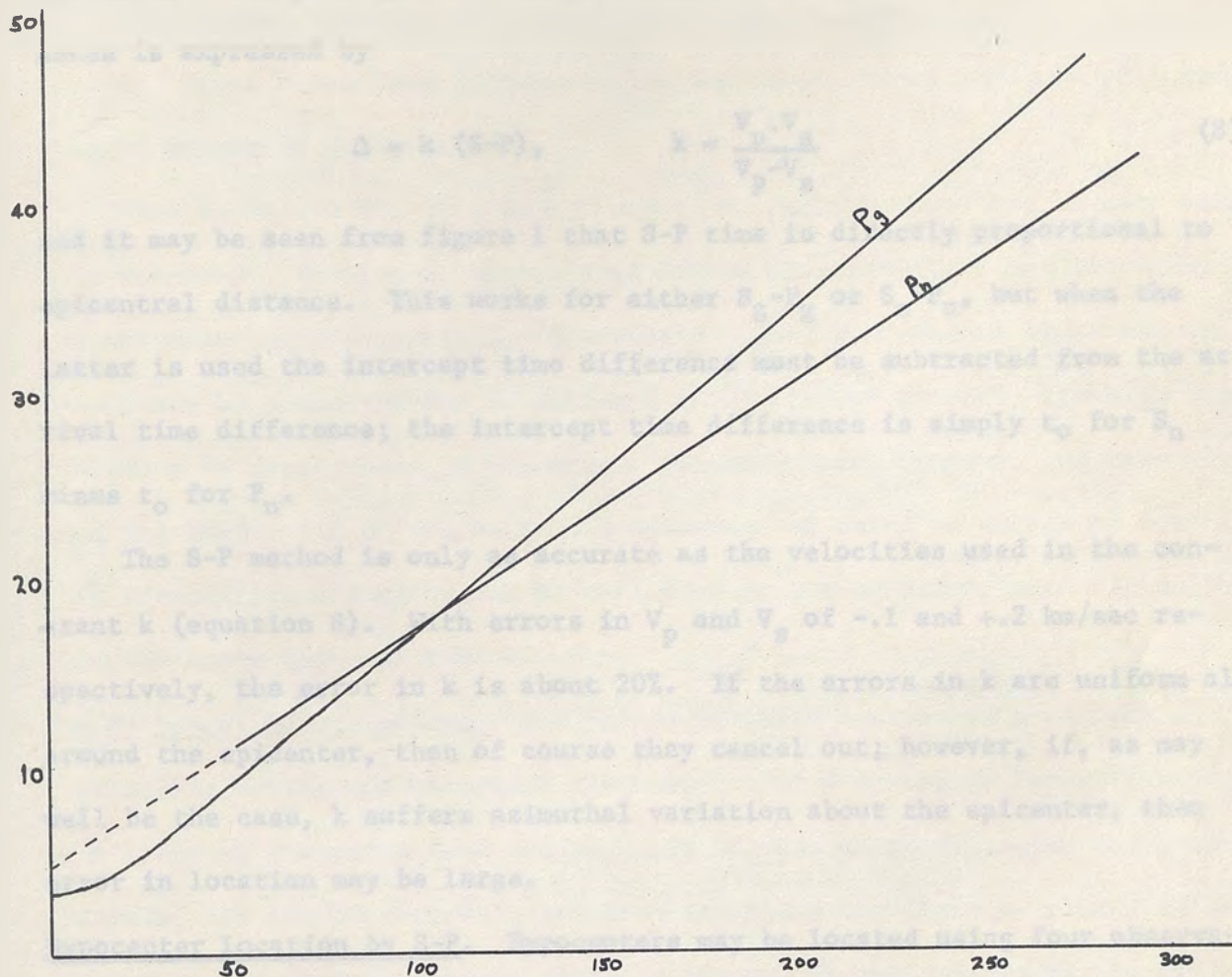


Fig. 2 Travel time curves for a focal depth of 15 km and ray-path diagram.

from three or more stations by S-P time differences, and then to lay off corresponding arcs on a map or globe; the intersection of the arcs marks the epicenter. The principle of finding epicentral distance by S-P time differences is expressed by

$$\Delta = k (S-P), \quad k = \frac{V_p \cdot V_s}{V_p - V_s} \quad (8)$$

and it may be seen from figure 1 that S-P time is directly proportional to epicentral distance. This works for either $S_g - P_g$ or $S_n - P_n$, but when the latter is used the intercept time difference must be subtracted from the arrival time difference; the intercept time difference is simply t_0 for S_n minus t_0 for P_n .

The S-P method is only as accurate as the velocities used in the constant k (equation 8). With errors in V_p and V_s of $-.1$ and $+.2$ km/sec respectively, the error in k is about 20%. If the errors in k are uniform all around the epicenter, then of course they cancel out; however, if, as may well be the case, k suffers azimuthal variation about the epicenter, then error in location may be large.

Hypocenter Location by S-P. Hypocenters may be located using four observations of $S_g - P_g$ times; this technique has been used in Japan by workers of the University of Tokyo in studies of aftershock sequences following large earthquakes (Earthquake Research Inst., 1950, pp. 387-392). Four or more portable instruments are moved into the field, close to and surrounding the epicenter of a major shock, and then the aftershocks are recorded. First the constant k of equation (8) must be determined, where D is the straight-line distance from hypocenter to station. To do this four observations at different locations are required, yielding four equations in four unknowns of the form

$$D_i^2 = (X-X_i)^2 + (Y-Y_i)^2 + Z^2 = k^2(S-P)_i^2, \quad (9)$$

$$i = 1, \dots, 4$$

where D_i is the distance to the hypocenter from the i th station, X_i and Y_i are the station's coordinates, and X , Y , Z are the coordinates of the hypocenter. After k has been determined for one event, three stations will suffice to determine X , Y , and Z .

This technique yields a unique solution, because there are no more data than unknowns. Because of this, large errors may arise if k and S-P times are not accurately determined. Systematic velocity variation about the epicenter may be accounted for by making k a function of azimuth, although this procedure is rarely seen in practice. Random errors, however, are unavoidable and impossible to evaluate; the advantage of using an excess of data is that inherent random error can be evaluated in the solution, once all systematic deviation has been removed.

The Method of Least Squares. The method of least squares is a well-known statistical device for obtaining the best fit of a system of linear equations to a group of scattered data points; this is also known as linear regression analysis, and the best-fitting solution is called the line (or plane) of regression. The method seeks to minimize the sum of the squares of the errors, i.e. the distances from data points to final regression plane. In the case of earthquake hypocenter location, an error is the difference between the calculated arrival time and the observed arrival time of a given phase at a given station.

In applying the method to earthquakes, a tentative epicenter is first found, usually on the basis of the S-P calculations described above; then a tentative origin time is assigned by subtracting traveltimes from arrival times at various stations, the traveltimes having been calculated using the tentative S-P epicenter. Any arbitrary depth of focus within the crust may

be assigned, and the solution will adjust it. The initial data for the method then consist of a first approximation of the hypocentral coordinates, which we wish to correct using least squares.

A series of n linear equations (one for each station) is written, each expressing the error in arrival time, E_i , at the i th station as a function of the unknown hypocentral coordinate adjustments X , Y , Z , T , and the residual F_i as expressed by

$$A_i X - B_i Y + C_i Z + D_i T - F_i = E_i \quad (10)$$

In this equation

$$A_i = \frac{\partial t_i^*}{\partial X_0^*}, \quad B_i = \frac{\partial t_i^*}{\partial Y_0^*}, \quad C_i = \frac{\partial t_i^*}{\partial Z_0^*}, \quad D_i = \frac{\partial t_i^*}{\partial t_0^*}, \quad F_i = t_i - t_i^*$$

where X_0^* , Y_0^* , Z_0^* , and T_0^* are the tentative hypocentral coordinates of latitude, longitude, depth, and origin time respectively, and t_i^* and t_i are the computed and observed arrival times at the i th station (t_i^* is computed on the basis of the tentative coordinates). The error E_i is just the observed arrival time less the computed and adjusted arrival time at the i th station. Next, the total derivative of the sum of the squares of the errors is set equal to zero,

$$d \left(\sum_{i=1}^n E_i^2 \right) = 0, \quad (11)$$

since we know that a function is extremal when its total derivative is zero. In this case we may find only a minimum value for $\sum E_i^2$ because it has no upper bound. Equation (11) yields the partial differential equation

$$\sum_{i=1}^n \left(E_i \frac{\partial E_i}{\partial X} + E_i \frac{\partial E_i}{\partial Y} + E_i \frac{\partial E_i}{\partial Z} + E_i \frac{\partial E_i}{\partial T} \right) = 0 \quad (12)$$

and since the partial derivatives must be zero when the function is minimal we get

$$\sum E_i \frac{\partial E_i}{\partial X} = \sum E_i \frac{\partial E_i}{\partial Y} = \sum E_i \frac{\partial E_i}{\partial Z} = \sum E_i \frac{\partial E_i}{\partial T} = 0. \quad (13)$$

These equations now generate the normal equations which may be solved for the adjustments X, Y, Z, T:

$$(X \ Y \ Z \ T) \cdot \begin{pmatrix} [A_i^2] & [A_i B_i] & [A_i C_i] & [A_i] \\ [A_i B_i] & [B_i^2] & [B_i C_i] & [B_i] \\ [A_i C_i] & [B_i C_i] & [C_i^2] & [C_i] \\ [A_i] & [B_i] & [C_i] & [1] \end{pmatrix} = ([F_i A_i] \ [F_i B_i] \ [F_i C_i] \ [F_i]) \quad (14)$$

where the brackets indicate summation from one to n. Finally the adjustments X, Y, Z, T are added to X_0^* , Y_0^* , Z_0^* , T_0^* respectively to yield the corrected hypocenter.

Certain elementary mathematical facts apply to the determination of depth of focus by least squares. We see that the elements of row 3 in the 4X4 matrix of equation (14) are those of row 4 multiplied by C_i , before summation. If the C_i are all the same then the two rows will be proportional, for in this case C_i can be brought out of the brackets, and the determinant of this matrix will be zero, in which case the system has no solution (Sokolnikoff and Redheffer, 1958, pp. 744-749). However, if the C_i are of different values ($C_i \neq C_2 \neq \dots C_k$) rows 3 and 4 will not be proportional, since in general $\Sigma(U_i \cdot V_i) \neq \Sigma U_i \cdot \Sigma V_i$, and the determinant will not be zero. For these reasons it is mandatory that P_g arrivals from various epicentral distances be used, giving different values of C_i . This may readily be seen because

$$C_i = \sin(\delta_i)/V_1 \quad (15)$$

where δ_i is the vertical angle of depression of the station-to-hypocenter ray (see figure 2). P_n arrivals will not alone suffice to determine depth, because the rate of change of P_n traveltime with depth is a constant for all

observation points; for P_n the value of C_1 is always $\cos(i_c)/V_1$. It would seem reasonable that for accurate solutions of focal depth, observations of P_g should lie on the noticeably curved part of the traveltime curve (see figure 2), where C_1 varies significantly with epicentral distance. P_n arrivals may be used at some stations, and the coefficients A_1 , B_1 , etc. will be calculated accordingly, using P_n velocities. However, since C_1 is constant at all stations, the use of P_n arrivals will not directly help determine depth; but they will further determine the other three coordinates, which indirectly should improve the quality of Z by reducing the standard error.

It must be stressed that least squares analysis requires the data (the coefficients A_1 , B_1 , C_1 , F_1) to be normally distributed with regard to their expected or true values (Crow, et al., 1960, p. 150). This means that systematic deviations must be eliminated from the data in order for results to be good. Each coefficient excepting F_1 contains the velocity as a factor; therefore if velocity varies systematically about the epicenter, this must be accounted for. In the event that systematic deviations exist but are unknown, the final solution may be in considerable error.

A least squares solution always has associated with it the standard deviation or error, which is a measure of the probable error in the calculation. This is given by

$$S = \sqrt{\frac{\sum E_i^2}{n-k-1}} \quad (16)$$

where E_i is the error at the i th station, n is the number of observations (stations), and k is the number of variables (Crow, et al., 1960, p. 174). It is seen from this equation that at least six observations are required for our hypocenter solution. There is also a formula for the standard error

of any calculated adjustment

$$S_j = S \sqrt{A_{jj}^{-1}} \quad (17)$$

where j denotes the column number of an element in the row vector (X Y Z T) and A_{jj}^{-1} is that element's diagonal component in the inverse normal matrix (the inverse of the 4X4 matrix of equation 14) (Crow, et al., 1960, p. 179). Unfortunately it is very difficult to solve for A_{jj}^{-1} symbolically: only numerical solutions are practical, and these only on an electronic computer. Thus the writer was not able to obtain an analytic expression for the standard error of focal depth.

The chief advantage of the least squares technique is its use of much data to improve results when a certain amount of random scatter is inherent in the data, as in seismic traveltimes. But, as has been stated, it will not remove systematic deviations, which for the case of hypocenter location must be eliminated by modifying the basic hypothesis of crustal structure. Disadvantages are the requirement of many stations--more than are usually available--and the lengthy, complicated calculations.

The Thirlaway Method. H. I. S. Thirlaway of Great Britain has recently proposed a variation on the P_g-P_n interval method of finding depth of focus, in which the P_g-P_n time difference for a given station is plotted against S_g-P_g . On this plot is drawn a line of surface focus events, corresponding to minimum P_g-P_n interval at any given range from the epicenter, the range being given implicitly by S_g-P_g . This procedure is supposed to work with one station, since the epicenter need not actually be located.

The essential idea in determining depth by means of the P_g-P_n interval is that at a given epicentral distance the time difference P_g-P_n is a function of depth of focus. One may see from equation (7) that the traveltime of P_n decreases as depth increases; P_g traveltime increases as h increases,

but at a much slower rate than P_2 time decreases. For example, at $h = 15$ km, $t = 150$ km, t changes 6 times as fast as when P_2 with depth, and this ratio increases rapidly with epicentral distance. From theoretical travel time curves for P_2 and P_3 one can determine directly the $P_2 - P_3$ interval for a surface focus at any epicentral distance. This may then be plotted on a graph against $P_2 - P_3$. Now actual observations of these values for an event are plotted and compared with the line of surface focus. Depth, h , may be calculated by the simple formula $h = (dt/dt) \Delta t$, where dt/dt is the rate of change of depth with $P_2 - P_3$ travel time, and Δt is "extra" $P_2 - P_3$ time above the line of surface focus. The theory will be discussed in more detail in Part II.

Thirlaway's method is extensively criticized in Western Special Report No. 1 (1961) by many outstanding seismologists. Chief problems in the application of the method are 1) the picking of the phases P_2 and P_3 , and 2) the variability in travel time curves from region to region. In many cases the onset of P_3 is difficult to pick on the record, and the velocity of P_3 is usually not well-known.

The writer has attempted to apply Thirlaway's method to nuclear shot Hardhat, detonated at the Nevada Test Site on February 15, 1962. Two very good recordings were used, which were made at Kanab, Utah, and Durango, Colorado at epicentral distances of 384 and 734 km respectively. The line of surface focus was calculated using an apparent velocity for P_2 of 3.6 km/sec and a velocity of 8.0 km/sec for P_3 (Ryall and Stuart, 1958, p. 5821); the velocity of P_3 was calculated to be 3.46 km/sec on the assumption of perfect elasticity. It may be seen from Figure 3 that at Kanab the readings plot very close to the line of surface focus, while at Durango there is some uncertainty. At Durango there are several possible picks on the record where P_3 might be picked; the obvious pick (number 1 on figure) is well above

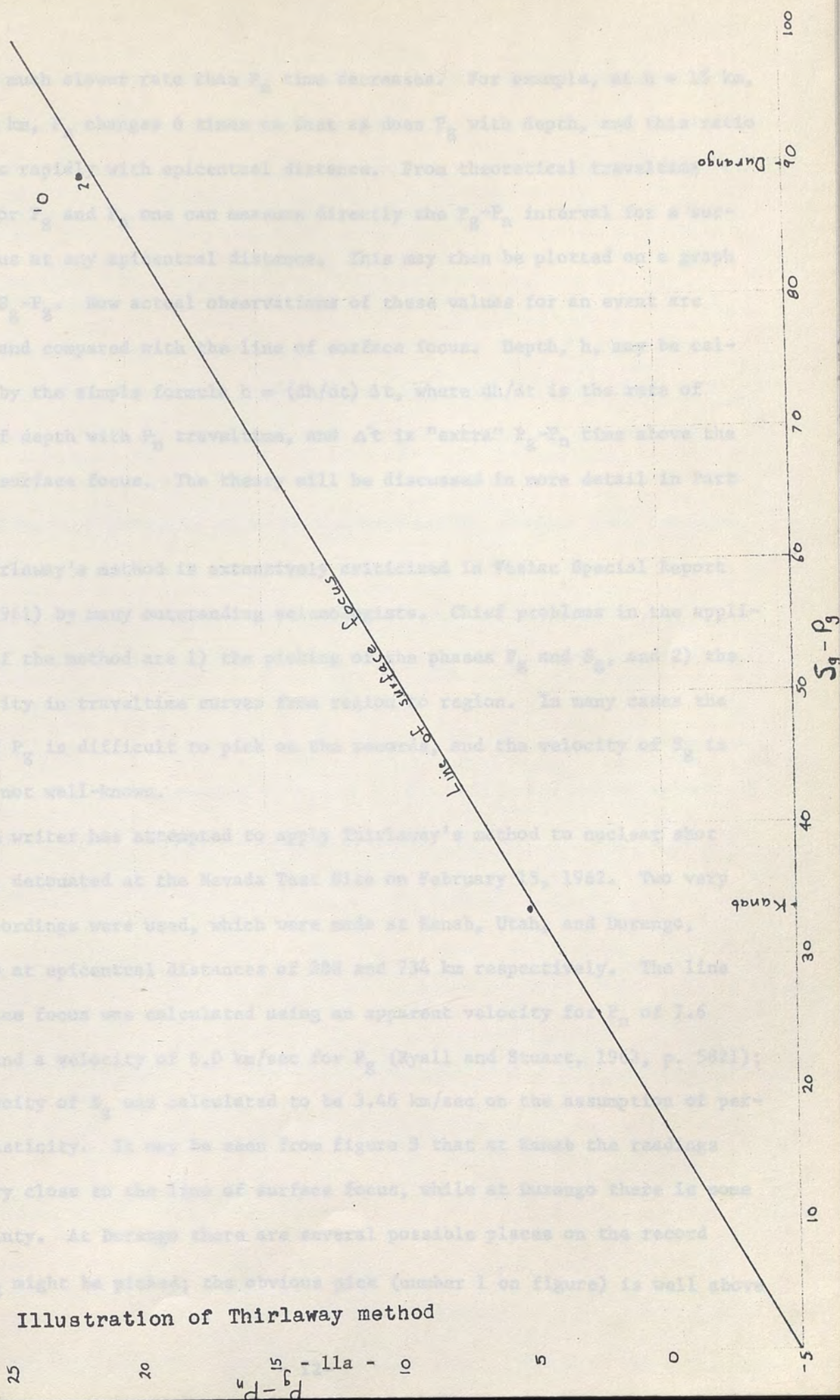


Fig. 3 Illustration of Thirlaway method

25 20 15 - 11a - 0 5 0 -5

but at a much slower rate than P_n time decreases. For example, at $h = 15$ km, $\Delta = 150$ km, P_n changes 6 times as fast as does P_g with depth, and this ratio increases rapidly with epicentral distance. From theoretical traveltime curves for P_g and P_n one can measure directly the $P_g - P_n$ interval for a surface focus at any epicentral distance. This may then be plotted on a graph against $S_g - P_g$. Now actual observations of these values for an event are plotted and compared with the line of surface focus. Depth, h , may be calculated by the simple formula $h = (dh/dt) \Delta t$, where dh/dt is the rate of change of depth with P_n traveltime, and Δt is "extra" $P_g - P_n$ time above the line of surface focus. The theory will be discussed in more detail in Part II.

Thirlaway's method is extensively criticized in Vesiac Special Report No. 1 (1961) by many outstanding seismologists. Chief problems in the application of the method are 1) the picking of the phases P_g and S_g , and 2) the variability in traveltime curves from region to region. In many cases the onset of P_g is difficult to pick on the records, and the velocity of S_g is usually not well-known.

The writer has attempted to apply Thirlaway's method to nuclear shot Hardhat, detonated at the Nevada Test Site on February 15, 1962. Two very good recordings were used, which were made at Kanab, Utah, and Durango, Colorado at epicentral distances of 288 and 734 km respectively. The line of surface focus was calculated using an apparent velocity for P_n of 7.6 km/sec and a velocity of 6.0 km/sec for P_g (Ryall and Stuart, 1963, p. 5821); the velocity of S_g was calculated to be 3.46 km/sec on the assumption of perfect elasticity. It may be seen from figure 3 that at Kanab the readings plot very close to the line of surface focus, while at Durango there is some uncertainty. At Durango there are several possible places on the record where P_g might be picked; the obvious pick (number 1 on figure) is well above

the surface-focus line, but a much weaker and earlier arrival (numbered 2) plots near the line. The partial success here (for Kanab readings) is due to the fact that crustal structure was determined by a refraction profile lying very close to our observation points (Ryall and Stuart, 1963). The difficulty in picking P_g at Durango may be typical at distances over a few hundred kilometers.

Thirlaway's method adds an extra variable to the basic P_g - P_n method--the velocity of S_g --and hence a greater probable error. In the above trial, it happened that the calculated velocity of S_g (3.46 km/sec) was very close to the observed velocity, 3.50 km/sec. But the agreement is not always this good, and in fact the ratio of P- to S-velocities may deviate from the ideal value of 1.73 by over 5% in some areas (Gutenberg, 1958, p. 32). Since the slope of the line of surface focus is proportional to the constant k of equation (8), it may be seen that a small error in V_{sg} will produce a much larger error in the line's slope.

It will be shown in Part III that the basic P_g - P_n method can be successfully applied if the velocities of P_g and P_n are well known and if epicentral distances are found independently of S_g .

II. THE P_g - P_n METHOD.

The fundamentals of using the P_g - P_n interval to determine depth of focus were stated in the description of the Thirlaway method. In the past, the application of the P_g - P_n method has not been entirely satisfactory, mainly because of insufficient knowledge of the crustal structure in the region of interest. In this section the theory of the P_g - P_n method will be developed mathematically, and assumptions will be clearly stated and explained, leading to an evaluation of the method's usefulness.

Wave velocities are of prime importance in the accurate determination of an earthquake focus, and in many cases the use of an average regional velocity is inadequate. In Nevada we now believe that the apparent velocity of P_n varies approximately sinusoidally with source-to-receiver azimuth (Ryall and Jones, 1964). This variation is consistent with theoretical calculations made on the basis of a Moho dipping about 2° east and striking $N 6^\circ W$; an eastward dip of a little over 2 degrees was found by Eaton (1963, p. 5803) from his Fallon to Eureka reversed refraction profile, and by Ryall and Stuart (1963, p. 5827) for a line running eastward from NTS. The apparent velocity of P_n in Nevada due to this dipping crust has been determined by Ryall (1964) to be

$$V = 7.86 - .24 \sin (\alpha + 6^\circ) \text{ km/sec} \quad (18)$$

where α is the azimuth of the epicenter-to-station ray in degrees east of north. This P_n velocity hypothesis is essential to the success of the P_g - P_n method as applied in Nevada.

In the mathematical derivation below, the following notation will be used:

t_{pn} = traveltime of P_n wave

t_{pg} = traveltime of P_g wave

t_{on} = intercept time of P_n

t_{og} = intercept time of P_g

V_1 = velocity of P_g

V_2 = velocity of P_n

i_c = critical angle of refraction at the Moho

Δ = epicentral distance

α = azimuth of the epicenter-to-station ray

ψ = angle of dip of the Moho

h = focal depth,

H = crustal thickness

From equations 6 and 7 we calculate that

$$\frac{\partial t_{pg}}{\partial h} = \frac{h}{V_1 (\Delta^2 + h^2)^{1/2}} \quad (19)$$

and

$$\frac{\partial t_{pn}}{\partial h} = -\frac{\cos i_c}{V_1} \quad (20)$$

For $h = 15$ km, $\Delta = 150$ km, $V_1 = 6.0$ km/sec, $V_2 = 8.0$ km/sec

$$\frac{\partial t_{pg}}{\partial h} \doteq +.017 \text{ sec/km, and } \frac{\partial t_{pn}}{\partial h} \doteq -0.11 \text{ sec/km}$$

and so for $h \leq 15$ km, $\Delta \geq 150$ km

$$\left| \frac{\partial t_{pg}}{\partial h} \right| \leq \frac{+1}{6} \frac{\partial t_{pn}}{\partial h}$$

From this result it is seen that for all practical purposes

$$\frac{\partial (t_{pg} - t_{pn})}{\partial h} \doteq -\frac{\partial t_{pn}}{\partial h}, \quad (21)$$

and

$$\delta (t_{pg} - t_{pn}) \doteq -\delta t_{pn} = \frac{+h \cos i_c}{V_1} \quad (22)$$

where

$$\delta(t_{pg} - t_{pn}) = (t_{pg} - t_{pn})_{\text{observed}} - (t_{pg} - t_{pn}) \Big|_{h=0}.$$

For a crust of constant thickness

$$(t_{pg} - t_{pn}) \Big|_{h=0} = \Delta \left[\frac{V_2 - V_1}{V_1 \cdot V_2} \right] - \delta T_0$$

where

$$\delta T_0 = (t_{on} - t_{og}) \Big|_{h=0}.$$

Thus

$$\delta(t_{pg} - t_{pn}) = (t_{pg} - t_{pn})_{\text{obs}} - \delta T_0 - \Delta k \quad (23)$$

where

$$k = \frac{V_2 - V_1}{V_2 \cdot V_1}.$$

Finally we obtain

$$h = \frac{V_1}{\cos i_c} \delta(t_{pg} - t_{pn}) \quad (24)$$

For the case of a dipping Moho, the apparent velocity \bar{V}_2 must be substituted into the preceding equations in place of V_2 ; V_2 varies with epicenter-to-station azimuth as given by equation 18. Also, δT_0 varies since t_{on} is proportional to crustal thickness. If the Moho is represented by a dipping plane, then

$$t_{on} = \frac{2 b \cos i_c}{V_1} \quad (25)$$

where b is the perpendicular distance from the Moho to the epicenter. In this particular case, where the Moho dips approximately 2 degrees, b and H are essentially the same (H is measured perpendicular to the surface). Therefore we find that

$$\delta T_0 = \frac{2 H \cos i_c}{V_1} - t_{og} \quad (26)$$

where H varies with epicentral position, increasing toward the east. Hence the final depth-of-focus formula for the case of a dipping Moho is

$$h = \frac{V_1}{\cos i_c} \left[(t_{pg} - t_{pn})_{obs} + \delta T_o - \Delta \left(\frac{\bar{V}_2 - V_1}{\bar{V}_2 \cdot V_1} \right) \right] \quad (27)$$

It is necessary to consider the error in an epicenter location caused by assuming the Moho to be horizontal when it is really a dipping surface, because a prerequisite to finding depth of focus is a good epicenter location. The travelttime equation of P_n for the case of a dipping Moho is

$$t = \frac{2 b \cos i_c}{V_1} - \frac{\sin (i_c - \beta)}{V_1}, \quad (28)$$

where β is the apparent dip of the Moho in the direction α . Using the relation

$$\sin \beta = \sin \psi \cdot \sin \alpha \quad (29)$$

and the approximation that $\cos \beta$ is equal to 1, one may easily show that

$$t = \frac{2 b \cos i_c}{V_1} + \frac{\Delta}{V_2 (1 - \sin \psi \sin \alpha)}, \quad (30)$$

which agrees well with Ryall's empirically determined velocity equation. Hence when an epicenter is erroneously located on the basis of a flat instead of a dipping Moho, the error in distance to the i th station is

$$\delta_i \Delta = V_2 (\sin \psi \sin \alpha_i) t_i, \quad (31)$$

where t_i and α_i are the travelttime and azimuth to that station. While it is very difficult to exactly calculate the error in the epicenter location from eq. (31), it would seem reasonable that if the azimuthal distribution of stations about the epicenter is fairly even, then the location error should be roughly

$$V_2 (\sin \psi) \bar{t}_i, \quad (32)$$

where \bar{t}_i is the average traveltime to the observing stations. This error in epicenter location will give rise to an error in depth of focus as calculated by equation (27). The factor k of equation (23) has an average value of about 0.040 sec/km, which means that each kilometer of error in epicentral distance (Δ) yields a time error of .04 seconds, resulting in a 0.36 km depth error when multiplied by $V_1/\cos i_c \approx 9$ km/sec.

Near-surface low-velocity material has an effect on the depth of focus as found by eq. 27 because P_g and P_n will be differentially delayed, making δT_o vary. If all natural seismic events are assumed to lie below the sedimentary layers, then the latter will have an effect only under the observing stations. We will now evaluate the effect of the weather layer thickness under a station upon the observed δT_o . For this purpose let us assume that the P_g ray makes a very small angle with the bottom of the weathered layer (see fig. 4). Then the intercept time for P_g is given by

$$t_{og} = \frac{h_w \cos i_2}{V_w}, \quad (33)$$

and for P_n by

$$t_{on} = \frac{(2H) \cdot \cos i_c}{V_1} - h_w \left[\frac{\cos i_c}{V_1} - \frac{\cos i_1}{V_w} \right] \quad (34)$$

where h_w and V_w are the thickness and velocity of the weathered layer. δT_o is just the difference of equations (34) and (33), from which it follows that the coefficient of h_w is

$$\frac{\cos i_1 - \cos i_2}{V_w} - \frac{\cos i_c}{V_1}, \quad (35)$$

which is the rate of change of δT_o with h_w . In a hypothetical case where V_w , V_1 , and V_2 are 2, 6, and 8 km/sec respectively, the above expression (35) is about - 0.10 sec/km; this is essentially the same as the rate of change of P_n

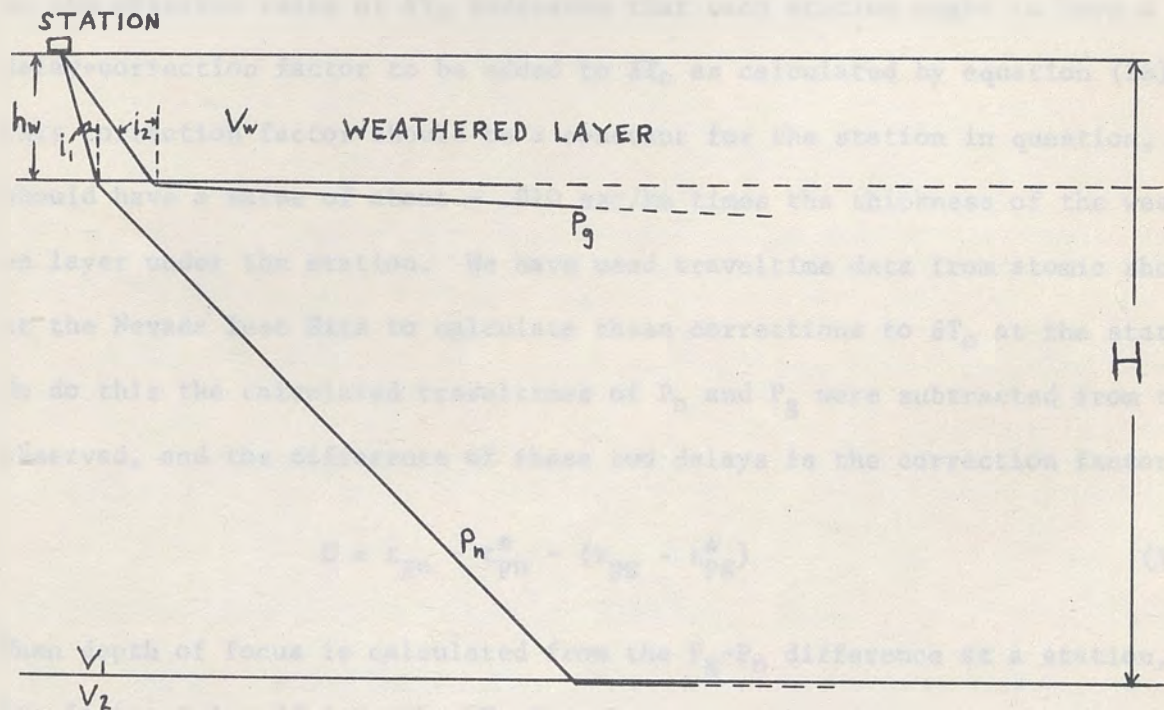


Fig. 4 Diagram showing effect of weathered layer on P_n and P_g .

traveltime with depth of focus. Therefore every kilometer of weathered layer not accounted for in a station correction will produce 1 kilometer of error in depth of focus as calculated from that station, assuming V_w is 2 km/sec. Actually, V_w may vary considerably, say from 2 to 4 km/sec, without affecting expression (35) seriously; if V_w is 4 km/sec then (35) becomes - .07 sec/km.

The above theoretical discussion of the effects of the weathered layer on the observed value of δT_0 indicates that each station ought to have a delay-correction factor to be added to δT_0 as calculated by equation (26). This correction factor should be a constant for the station in question, and should have a value of about - .010 sec/km times the thickness of the weathered layer under the station. We have used traveltime data from atomic shots at the Nevada Test Site to calculate these corrections to δT_0 at the stations. To do this the calculated traveltimes of P_n and P_g were subtracted from the observed, and the difference of these two delays is the correction factor C:

$$C = t_{pn} - t_{pn}^* - (t_{pg} - t_{pg}^*) \quad (36)$$

When depth of focus is calculated from the P_g - P_n difference at a station, the factor C is added to the δT_0 for the epicenter under consideration. While the absolute values of these C's will be somewhat too large on account of our disregarding shot point delays, it is assumed that their relative values (differences) are nearly correct; hence agreement of depths of focus calculated from different stations for a given event should be improved. The corrections calculated for Reno, Crown, Tonopah, and Eureka respectively are -0.4, 0.0, -0.3, and -0.1 second. The value for Reno was obtained directly by equation (36), but the other three were found using a P_g delay calculated from the expression

$$D_{pg} = D_{pn} \cdot \frac{(\cos i_2)/V_w}{(\cos i_c)/V_1 - (\cos i_1)/V_w}, \quad (37)$$

where D_{pg} and D_{pn} are the P_g and P_n delays. This had to be done because in most cases P_g arrivals were entirely off-scale at Crown, Tonopah, and Eureka. Furthermore, the calculated and observed P_g delays agreed perfectly at Reno.

III. APPLICATION OF THE METHOD TO SOME NEVADA EARTHQUAKES.

This section consists of a compilation and analysis of some epicenters and depths of focus of Nevada earthquakes which occurred between November 1963 and June 1964. However, before discussing the results of calculations, the criteria and problems involved in picking P_g arrivals on the seismograms will be reviewed briefly. The phase P_g generally has greater amplitude and shorter period than P_n , and in many cases there is no problem in identification of this phase on the records. However, for small earthquakes and on some types of instruments, P_g is a very weak arrival and does not stand out at all in the P-wave train. The readability of P_g on the seismogram is largely dependent on the frequency response of the seismometer receiving it. Near-regional shocks at epicentral distances of 100 to 300 kilometers seem to have most of their energy in the frequency range 3 to 4 cycles per second. Some seismometers are insensitive to these frequencies. For example, the Reno short-period Sprengnether instrument has its peak response near $\frac{1}{2}$ cps., and it is down about 65% from peak magnification at 4 cps.; hence Reno data seldom appears in depth of focus calculations. However, the North Reno station, installed in April 1964, has much better high-frequency response. Records best showing P_g were those from Crown Mine, where a short-period Benioff was in use. Tonopah also gave good recordings of P_g . It should be noted that the Reno Sprengnether has a very low magnification of 8000, whereas the other two stations have gains of 100,000 or more. The U. S. Coast and Geodetic Survey's station at Eureka uses a high-magnification instrument with good high-frequency response, hence Eureka records were useful in focal depth calculations. Figure 5 shows the location of all the above stations.

It must be noted here that the P_g - P_n method will not work in practice when the epicenter is less than the critical distance (fig. 1) from the sta-

tion observing the P_g-P_n interval. In this case P_n cannot usually be picked as a second arrival, because it will be masked at small distances by the higher-amplitude phase P_g .

In Table I epicenters and depths of focus have been listed for 28 Nevada earthquakes which occurred between the dates November 6, 1963 and June 16, 1964. Origin time is given in Greenwich Mean Time, the epicentral coordinates are in degrees and hundredths, epicentral distance (Δ) and focal depth (h) in kilometers, azimuth (Az.) of the epicenter-to-station ray in degrees east of north, and P_g-P_n time in seconds; the station symbols are R for Reno, N for North Reno, C for Crown Mine, E for Eureka, and T for Tonopah. A dash in the P_g-P_n column indicates that P_g was not readable at that station. Figure 5 shows the epicenters listed in Table I.

The main objective of this compilation was to determine whether or not depths of focus calculated from the P_g-P_n intervals at different stations agree for a given event. Since P_g-P_n intervals cannot be read more accurately than ± 0.1 second, any two observations may have a combined relative error of ± 0.2 second; from this it follows that the depths calculated may differ by 2 km and be within seismogram reading error since the rate of change of P_g-P_n time with depth is about 0.1 sec/km. If the basic crustal structure hypothesis is correct, then the depths ought to agree within approximately 2 km. Actually ten of the earthquakes in Table I show depth agreement within 2 km or better, and seventeen within 4 km or better. The earthquakes having very poor depth agreement will be given special attention below.

Tonopah earthquake series. A series of earthquakes occurred 15 km east of Tonopah on November 16, 1963, and the focal depths calculated at Crown Mine and Eureka were 14 and 13 kilometers respectively for the four listed events.

Actually about 25 earthquakes were recorded at Tonopah on November 16, but only the four shown were large enough to be recorded well at Crown Mine and Eureka; none were recorded at Reno. S-P time at Tonopah indicated that the hypocentral distance there was 23 km; since the epicentral distance was 15 km, the depth of focus was calculated to be 17 km. The good agreement of depths calculated by the two methods, S-P and P_g-P_n , indicates that the epicenter is accurate and that the crustal model is true. The epicenter used for these Tonopah shocks is an average of the one given by the U. S. Coast and Geodetic Survey with the one found by S-P times at Tonopah, Crown Mine, and Eureka. The epicenter found by Ryall's computer program (Ryall and Jones, 1964) was greatly in error on account of there being no radio time corrections at Crown Mine for over a week; hence S-P location was used since it does not require absolute timing.

Walker Lake series. Another series of earthquakes occurred at the southern end of Walker Lake between March 22 and April 12, 1964. The first eight events (March 22 to March 30) show quite good focal depth agreement at Reno, Crown, and Tonopah, however the two following events are not as good, showing three negative values. All of the Walker Lake events had negative depths when initially calculated using a value of 4.2 seconds for δT_0 , which was assigned on the basis of the Ryall-Jones crustal model. However, δT_0 was increased by 1.3 second in the Walker Lake area for reasons given below.

The Walker Lake crustal anomaly. An anomaly in crustal structure in the Walker Lake area became apparent to the writer when the initially-calculated depths of focus for the Walker Lake events were all negative. Their good agreement at the three stations indicated that the distances and velocities used were correct, and hence the error had to be in the parameter δT_0 , which is constant for a given epicenter. Apparently δT_0 is in reality larger than the 4.2 seconds predicted by the westward extension of Ryall's crustal model.

Since $\delta T_0 = t_{on} - t_{og}$, an increase in t_{on} is implied, corresponding to an increase of crustal thickness at the epicenter, H_{ep} , because

$$t_{on} = \frac{2H \cos i_c}{V_1} + \frac{H_{ep} \cos i_c}{V_1} . \quad (38)$$

Ryall's crustal model indicates t_{on} is 5.0 seconds, or $H = 23$ km, at Walker Lake, but it is significant that this model does not include or fit with the data of Eaton's Fallon to Owens Valley refraction line. Eaton finds that the crust thickens to 45 km north of Owens Valley (1963, p. 5803); furthermore, he says that most of this thickening occurs within 50 km south of Fallon. The writer used Eaton's observation of $P_M P$ (reflection off the Moho) at a distance of 92 km from Fallon to calculate a crustal thickness of 35 km for a point 45 km south of Fallon (Eaton, 1963, p. 5798); this was done on the assumption of a single-layer crust with velocity 6 km/sec. This crustal thickness of 35 km was assumed for central Walker Lake, 40 km to the south. On this basis t_{on} , hence δT_0 , at Walker Lake was increased by 1.3 second, which made positive all but three of the focal depths for the Walker Lake events. Eaton also finds that the crust thickens abruptly about 40 km west of Fallon from his Fallon to San Francisco refraction profile (1963, p. 5804).

Further evidence for the local crustal thickening in the Walker Lake area is supplied by data from earthquakes at or near its supposed eastern boundary (see fig. 5). Epicenters shown as solid circles have been located using stations only to the east (Eureka, Crown, and Tonopah), and focal depths calculated for them agree fairly well, indicating that the Ryall-Jones crustal model is good east of the boundary. However, the half-shaded epicenters, located using North Reno, showed strong disagreement of focal depths; these are the last six entries in Table I. It is seen that the North Reno depths are large and negative, while those for Tonopah and Crown are less negative or are positive. Apparently the $P_g - P_n$ interval is consistently a-

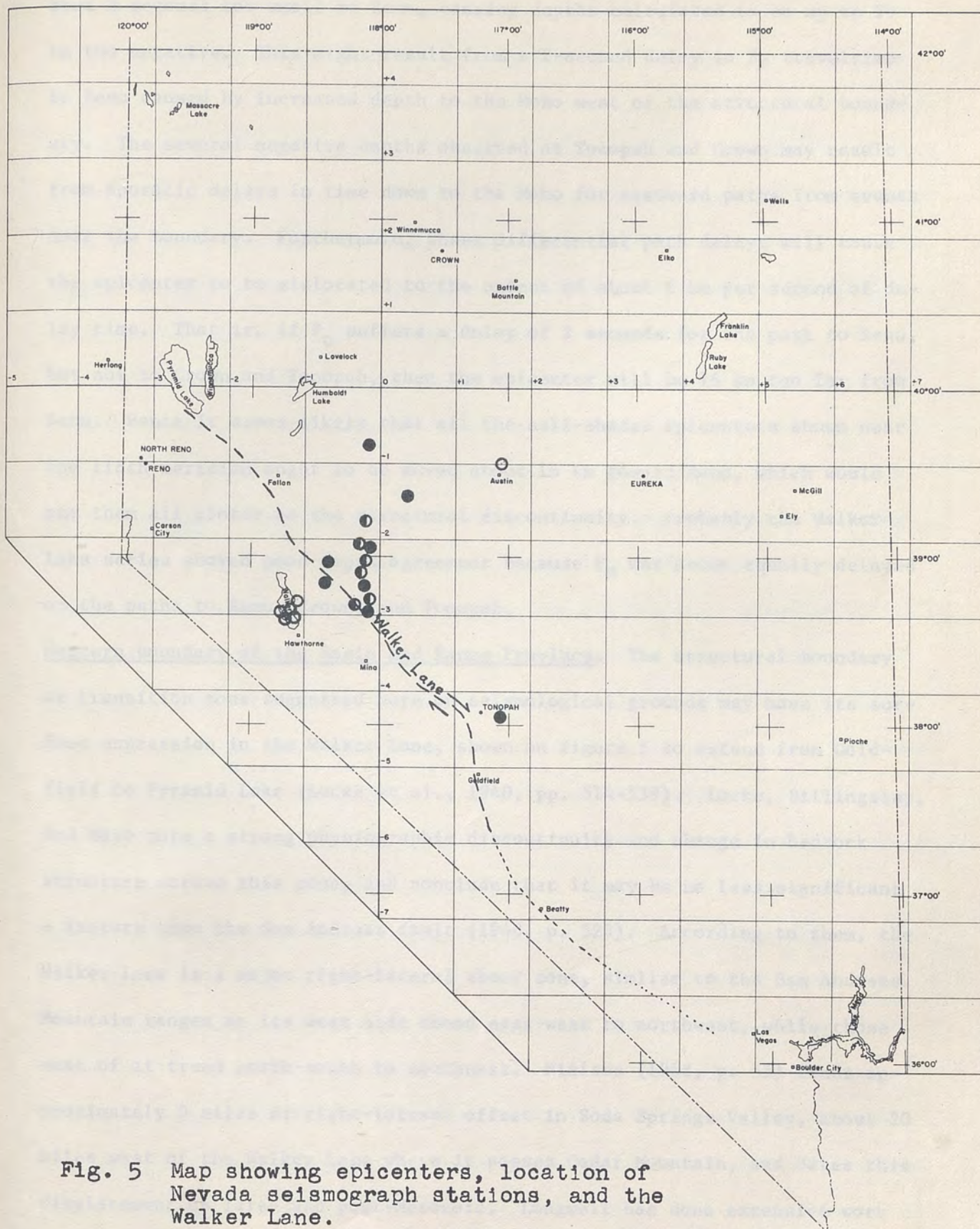


Fig. 5 Map showing epicenters, location of Nevada seismograph stations, and the Walker Lane.

bout 2 seconds too small at Reno, causing depths calculated to be up to 20 km too negative. This might result from a 2-second delay in P_n traveltime to Reno caused by increased depth to the Moho west of the structural boundary. The several negative depths observed at Tonopah and Crown may result from sporadic delays in time down to the Moho for eastward paths from events near the boundary. Furthermore, these differential path delays will cause the epicenter to be mislocated to the extent of about 8 km per second of delay time. That is, if P_n suffers a delay of 2 seconds for the path to Reno, but not to Crown and Tonopah, then the epicenter will be 16 km too far from Reno. Hence it seems likely that all the half-shaded epicenters shown near the 118th meridian ought to be moved about 16 km toward Reno, which would put them all closer to the structural discontinuity. Probably the Walker Lake series showed good depth agreement because P_n was about equally delayed on the paths to Reno, Crown, and Tonopah.

Western boundary of the Basin and Range Province. The structural boundary or transition zone suggested here on seismological grounds may have its surface expression in the Walker Lane, shown on figure 5 to extend from Goldfield to Pyramid Lake (Locke et al., 1940, pp. 514-539). Locke, Billingsley, and Mayo note a strong physiographic discontinuity and change in bedrock structure across this zone, and conclude that it may be no less significant a feature than the San Andreas fault (1940, p. 523). According to them, the Walker Lane is a major right-lateral shear zone, similar to the San Andreas. Mountain ranges on its west side trend east-west to northwest, while those east of it trend north-south to northeast. Nielsen (1962, p. 53) finds approximately 9 miles of right-lateral offset in Soda Springs Valley, about 20 miles west of the Walker Lane where it passes Cedar Mountain, and dates this displacement as late- and post-Mesozoic. Longwell has done extensive work

on the Las Vegas Valley shear zone, apparently part of the Walker Lane, and infers about 25 miles of right-lateral offset there, also late- and post-Mesozoic (1960, p. 197); fold axes, thrust traces, and strikes of tilted beds are sharply bent into truncated S-curves as they approach the shear zone from either side. Right-lateral faulting is seen at Bare Mountain, a little southeast of Beatty (Cornwall and Kleinhampl, 1964, p. J15). Longwell also finds that present range trends on either side of the Walker Lane are parallel to much earlier structural features of folding and thrusting (1950, p. 426).

Gianella and Callaghan connected the 1932 Cedar Mountain earthquake to a major shear zone corresponding to the Walker Lane (the name was not yet in use), and described in detail the large area of en echelon and rift faults extending from Cedar Mountain to Gabbs Valley, a distance of about 30 miles (1934, pp. 1-22). In addition, they causally relate the right-lateral displacements on the Walker Lane to those on the San Andreas. Slemmons (1956) found right-lateral displacements of up to 12 feet at Fairview Peak after the earthquake which occurred there on December 16, 1954; Fairview Peak is about 30 miles north of the Walker Lane in Gabbs Valley. It should be noted that the Pleasant Valley earthquake of 1915 and the Dixie Valley earthquake in 1954 produced essentially no strike slip faulting, and that they occurred far away from the Walker Lane (Richter, 1958, pp. 504-513). The area from Fairview Peak to Cedar Mountain is currently one of high seismicity, as may be seen on figure 5, and has been so ever since the 1932 earthquake.

From all of these studies, it is concluded that the Walker Lane is a structural feature of great importance, and that it may be a fundamental boundary between two crustal provinces or blocks. This conclusion is supported by the apparent abrupt increase in crustal thickness west of the lane, and by geological data given above. This view agrees with that of Locke, et

al. (1940, p. 523), who say that the Walker Lane may mark the eastern limit of the Sierra Nevada structural province with its granitic core. Furthermore, the crustal model of Ryall and Jones is seen to be valid east, but not west of the Walker Lane. Therefore, for seismological purposes, the Walker Lane might be defined as the western boundary of the Basin and Range Province in Nevada.

| Date | Time | Lat | Long | Depth | Magnitude | Location |
|---------|------------|-------|--------|-------|-----------|----------|
| Nov. 27 | 11:58:41.7 | 38.01 | 117.10 | 10 | 2.5 | ... |
| Nov. 28 | 12:38:59.7 | 38.21 | 117.05 | 10 | 2.5 | ... |
| Nov. 18 | 15:24:24.4 | 38.26 | 117.06 | 10 | 2.5 | ... |
| Nov. 19 | 15:25:05.0 | 38.26 | 117.07 | 10 | 2.5 | ... |
| Nov. 20 | 20:44:46.7 | 38.26 | 117.13 | 10 | 2.5 | ... |
| Nov. 21 | 00:01:42.8 | 38.27 | 117.14 | 10 | 2.5 | ... |
| Nov. 18 | 03:41:13.7 | 38.28 | 117.21 | 10 | 2.5 | ... |
| Nov. 21 | 11:52:36.8 | 38.25 | 117.13 | 10 | 2.5 | ... |
| Nov. 1 | 04:02:18.4 | 38.26 | 117.01 | 10 | 2.5 | ... |
| Nov. 22 | 01:30:12.0 | 38.26 | 117.20 | 10 | 2.5 | ... |

* T_p measured by ... about ...

TABLE I

Epicenters and Depths of Focus

| Date | Origin Time | Epicenter | Sta. | | Az. | $P_g - P_n$ | h |
|---------|-------------|-----------|------|-----|-----|-------------|------|
| Nov. 6 | 11:17:35.9 | 38.52 | E | 143 | 42 | 3.0 | 28 |
| | | 117.09 | C | 257 | 351 | 7.2 | 23 |
| Nov. 8 | 07:44:23.1 | 38.69 | T | 101 | 133 | 1.4 | 19 |
| | | 118.07 | E | 201 | 64 | 3.0 | 4 |
| | | | C | 240 | 11 | 6.5 | 18 |
| Nov. 16 | 11:58:41.7 | 38.07 | E | 188 | 30 | 3.0 | 13 |
| | | 117.08 | C | 306 | 352 | 8.0 | 14 |
| Nov. 16 | 12:34:39.1 | 38.07 | E | 188 | 30 | 3.0 | 13 |
| | | 117.08 | C | 306 | 352 | 8.0 | 14 |
| Nov. 16 | 12:56:35.2 | 38.07 | E | 188 | 30 | 3.0 | 13 |
| | | 117.08 | C | 306 | 352 | 8.0 | 14 |
| Nov. 16 | 14:23:44.3 | 38.07 | E | 188 | 30 | 3.0 | 13 |
| | | 117.08 | C | 306 | 352 | 8.0 | 14 |
| Nov. 24 | 20:44:54.9 | 38.84 | T | 116 | 137 | 0.7 | 7 |
| | | 118.13 | E | 199 | 68 | 3.5 | 9 |
| | | | C | 225 | 13 | 4.5 | 6 |
| Dec. 9 | 00:42:28.0 | 38.87 | T | 138 | 130 | 1.2 | 14 * |
| | | 118.44 | E | 223 | 72 | 4.1 | 17 |
| | | | C | 230 | 19 | 5.0 | 15 |
| Dec. 18 | 03:21:33.5 | 38.98 | T | 143 | 135 | 0.5 | 6 * |
| | | 118.38 | C | 216 | 19 | 3.0 | 5 |
| | | | E | 214 | 75 | 2.0 | 0 |
| Dec. 24 | 17:52:38.6 | 38.73 | T | 109 | 132 | --- | |
| | | 118.14 | E | 204 | 66 | 2.0 | 6 * |
| | | | C | 237 | 12 | 3.2 | 2 |
| Jan. 1 | 19:17:28.1 | 39.32 | T | 148 | 159 | 0.4 | - 5 |
| | | 117.81 | C | 167 | 8 | 1.5 | 1 |
| | | | E | 159 | 83 | 1.5 | 6 |
| Mar. 22 | 15:56:17.9 | 38.69 | R | 137 | 314 | 1.0 | 4 * |
| | | 118.63 | T | 141 | 119 | 0.5 | 5 |
| | | | C | 253 | 26 | 4.6 | 7 |

* T_0 increased by 1.3 second over that given by the Ryall-Jones crustal model.

TABLE I (cont'd)

| Date | Origin Time | Epicenter | Sta. | | Az. | $P_g - P_n$ | h |
|---------|-------------|-----------|------|-----|-----|-------------|-------|
| Mar. 22 | 16:30:53.3 | 38.71 | R | 137 | 314 | 1.0 | 4 * |
| | | 118.63 | T | 141 | 119 | 0.5 | 5 |
| | | | C | 253 | 26 | --- | |
| Mar. 23 | 15:32:53.4 | 38.66 | R | 137 | 314 | 0.6 | 0 * |
| | | 118.67 | T | 142 | 119 | 0.5 | 4 |
| | | | C | 258 | 26 | 4.2 | 1 |
| Mar. 24 | 23:57:07.3 | 38.68 | R | 132 | 317 | 1.0 | 5 * |
| | | 118.75 | T | 148 | 117 | 0.6 | 4 |
| | | | C | 258 | 23 | 4.5 | 4 |
| Mar. 25 | 04:37:27.3 | 38.71 | R | 137 | 314 | --- | * |
| | | 118.62 | T | 141 | 116 | 0.1 | 2 |
| | | | C | 253 | 26 | 4.2 | 3 |
| Mar. 27 | 13:51:20.2 | 38.71 | R | 137 | 314 | --- | * |
| | | 118.61 | T | 141 | 116 | 0.5 | 5 |
| | | | C | 253 | 26 | 4.2 | 3 |
| Mar. 28 | 23:05:59.3 | 38.68 | R | 137 | 314 | --- | * |
| | | 118.76 | T | 141 | 116 | 0.3 | 3 |
| | | | C | 253 | 26 | 4.3 | 3 |
| Mar. 30 | 09:47:33.8 | 38.66 | R | 131 | 319 | --- | * |
| | | 118.79 | T | 150 | 115 | 0.6 | 5 |
| | | | C | 263 | 24 | 4.3 | 1 |
| Apr. 11 | 03:25:04.5 | 38.69 | N | 132 | 317 | 0.1 | - 3 * |
| | | 118.81 | T | 154 | 116 | 0.6 | 4 |
| | | | C | 260 | 25 | 4.0 | - 1 |
| Apr. 12 | 08:51:19.4 | 38.66 | N | 137 | 317 | --- | * |
| | | 118.77 | T | 148 | 116 | 0.6 | 5 |
| | | | C | 262 | 23 | 4.0 | - 1 |
| Apr. 12 | 09:24:35.2 | 38.67 | N | 132 | 318 | 0.5 | 1 * |
| | | 118.83 | T | 153 | 115 | 0.5 | 3 |
| | | | C | 262 | 25 | --- | |
| Apr. 14 | 10:56:40.7 | 38.95 | T | 123 | 143 | 0.7 | 5 |
| | | 118.07 | N | 167 | 294 | 0.5 | -20 |
| | | | C | 211 | 12 | 2.2 | -10 |
| May 25 | 09:11:29.3 | 39.62 | C | 140 | 18 | 0.7 | 2 |
| | | 118.05 | N | 153 | 267 | 0.5 | -15 |
| | | | T | 187 | 157 | 2.0 | - 5 |

TABLE I (cont'd)

| Date | Origin Time | Epicenter | Sta. | | Az. | $P_g - P_n$ | h |
|---------|-------------|-----------|------|-----|-----|-------------|-----|
| June 4 | 02:55:14.6 | 39.01 | T | 129 | 143 | 0.6 | 3 |
| | | 118.10 | N | 162 | 292 | 0.5 | -18 |
| | | | C | 206 | 13 | --- | |
| June 10 | 02:50:50.2 | 39.20 | T | 145 | 149 | --- | |
| | | 118.06 | N | 158 | 285 | 1.0 | -13 |
| | | | C | 185 | 14 | 2.5 | - 2 |
| June 14 | 01:46:13.5 | 39.03 | T | 131 | 144 | 0.5 | 1 |
| | | 118.09 | N | 162 | 291 | 0.6 | -17 |
| | | | C | 203 | 13 | 3.0 | 0 |
| June 16 | 22:19:07.6 | 39.38 | C | 165 | 16 | 3.0 | 13 |
| | | 118.07 | N | 153 | 277 | --- | |
| | | | T | 164 | 153 | 0.7 | -10 |

REFERENCES

- Cornwall, Henry R., and Frank J. Kleinhampl
 1964. "Geology of the Bullfrog Quadrangle and Ore Deposits Related to Bullfrog Hills Caldera, Nye County, Nevada, and Inyo County, California" U.S.G.S. Prof. Paper 454-J.
- Crow, Edwin L., Frances A. Davis, and Margaret W. Maxfield
 1960. Statistics Manual, Dover Publications Inc., New York.
- Earthquake Research Institute
 1950. "Observations of Aftershocks Carried out in Imaichi District, Tochigi Prefecture" Bull. of the Earthquake Research Institute, Tokyo, 28: pt. 3-4, 387-392.
- Eaton, Jerry P.
 1963. "Crustal Structure from San Francisco, California, to Eureka, Nevada, from Seismic-Refraction Measurements" Journal of Geophysical Research, 68: 5789-5806.
- Gianella, V. P. and E. Callaghan
 1934. "The earthquake of December 20, 1932, at Cedar Mountain, Nevada, and its Bearing on the Genesis of Basin-Range Structure" Jour. of Geol. 42:1: 1-22.
- Gutenberg, Beno
 1959. Physics of the Earth's Interior, Academic Press, New York.
- Locke, A., P. Billingsley, and E. B. Mayo
 1940. "Sierra Nevada Tectonic Pattern" Bull. Geol. Soc. Amer., 51: 513-540.
- Longwell, C. R.
 1950. "Tectonic Theory Viewed from the Basin Ranges" Bull. Geol. Soc. Amer., 61: 413-434.
- Nielsen, Richard L.
 1962. "Right-lateral Strike-slip Faulting in West-Central Nevada", Abs. in Geol. Soc. Am. Special Paper 73.
- Pakiser, L. C., and others
 1963. "Symposium on the Structure of the Western United States" Jour. Geophys. Res., 68: 5747-5849.
- Richter, Charles F.
 1958. Elementary Seismology, W. H. Freeman and Co., San Francisco.
- Ryall, Alan and A. E. Jones
 1964. "Computer Program for Automatic Processing of Basin and Range Seismic Data" Bull. Seis. Soc. Amer., in press.
- Ryall, Alan S. and David Stuart
 1963. "Travel Times and Amplitudes from Nuclear Explosions, Nevada Test Site to Ordway, Colorado" Jour. Geophys. Res., 68: 5821-5835.

REFERENCES (cont'd)

Slemmons, David B.

1957. "Geological Effects of the Dixie Valley-Fairview Peak, Nevada, Earthquakes of December 16, 1954" Bull. Seis. Soc. Amer., 47: 353-376.

Sokolnikoff, I. S. and R. M. Redheffer

1958. Mathematics of Physics and Engineering, McGraw-Hill Book Co., Inc., New York.

Vesiac staff

1961. "A Consideration of H. I. S. Thirlaway's 'Depth of Focus Discrimination within the Crust at First-Zone Distances'" Vesiac Special Advisory Report Number 1, Inst. of Technology, Univ. of Mich., Ann Arbor.